Probing the Contributions of Interior and Exterior Channels of Nanofillers towards Enhanced Separation Performance of Thin-Film Nanocomposite Reverse Osmosis Membrane

Jun Yin[a,b], Zhe Yang[a,c*], Chuyang Y. Tang[c] and Baolin Deng[a*]

[a] Department of Civil and Environmental Engineering, University of Missouri, Columbia, Missouri, 65211, United States

[b] Nanova Environmental Inc., Columbia, Missouri, 65211, United States

[c] Department of Civil Engineering, the University of Hong Kong, Pokfulam, Hong Kong, SAR, P. R. China

[*] Corresponding Authors.

Phone: (+852) 2857 8470; E-mail address: zheyang@connect.hku.hk

Phone: (+1) 573 882 0075; Email: dengb@missouri.edu

ABSTRACT

Thin-film nanocomposite membranes (TFN) have been increasingly applied to seawater desalination and wastewater reclamation. Despite their potential to overcome the longstanding permeability-selectivity tradeoff, the underlying water transport mechanisms through TFN membranes have not been fully understood. In this study, we conducted an in-depth analysis of water transport through the TFN membranes incorporating nanoparticles of systematically changed properties (hydrophilic vs. hydrophobic and porous vs. nonporous). For the first time, we were able to resolve the respective contributions towards enhanced membrane performance by the exterior and interior channels of the nanofillers based on direct experimental evidence. Incorporating solid hydrophobic nanofillers showed little enhancement effect on water flux. In contrast, exterior channels created by hydrophilic nanofillers and interior channels of porous nanofillers had water flux enhancement of 26.9% and 18.3%, respectively, under similar particle loading conditions. Furthermore, the combined effects of both exterior and interior channels resulted in 51.9% flux enhancement. Our work provides mechanistic insights into the formation and transport mechanisms involved in TFN membranes, which lay a solid foundation for optimizing these membranes for desalination and water reuse.

TOC art

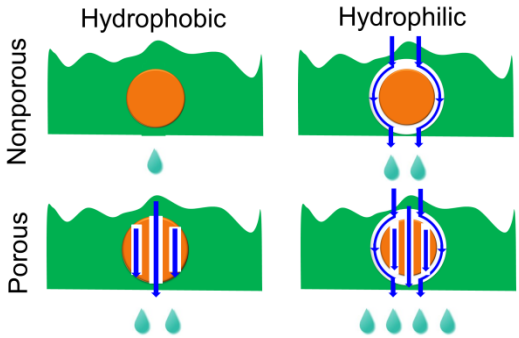

INTRODUCTION

Desalination and water reuse based on reverse osmosis (RO) are promising to address the challenge of water shortage globally.[1-3] To date, thin-film composite membrane (TFC) is the core of RO process, thanks to its high NaCl rejection (>99%), wide pH tolerance, high packing density, and excellent mechanical strength.[4, 5] The state-of-the-art TFC membrane is formed by an interfacial polymerization (IP) reaction between a diamine monomer in the aqueous phase and an acyl chloride monomer in the organic phase that generates an ultra-thin polyamide rejection layer of 10-200 nm on a microporous ultrafiltration substrate.[6, 7] Nevertheless, the separation performance of TFC membrane, i.e., water permeance and water/solute selectivity, is greatly constrained by the permeability-selectivity tradeoff, also known as the upper bound.[6, 8, 9]

Incorporation of nanomaterials into polyamide rejection layer can greatly improve membrane water permeance without sacrificing its selectivity.[10] Hoek et al.[11, 12] pioneered the concept of incorporating microporous zeolite nanoparticles (NPs) into a polyamide layer to increase its membrane water flux. Their seminal work on thin film nanocomposite (TFN) membranes has inspired many other researchers to explore over the past decade the incorporation of various porous nanofillers (e.g., metal-organic-frameworks (MOFs),[13, 14] aquaporins,[15, 16] and covalent-organic-frameworks.[17, 18] By comparing the TFN membranes loaded with porous MCM-41 vs. nonporous silica NPs, Yin et al.[19] confirmed that the interior

channels contribute significantly to the final membrane water flux. In a more recent study, Yang et al.[20] revealed the creation of interfacial channels between hydrophilic silver NPs and the polyamide matrix (i.e., exterior channels), which tripled the membrane water permeance under optimized conditions. Yang's observation explains why the incorporation of nonporous hydrophilic nanofillers reported in the literature (e.g., silver,[20, 21] and titanium oxides[22, 23]) can also significantly enhance membrane water transport properties. Nevertheless, the relative contribution of interior (the internal pores of NPs) and exterior channels (gaps between NPs and polymer) to membrane water flux and the underlying water transport mechanism of TFN membranes still remain unclear.[11, 20]

This study presents a systematic framework to resolve the roles of interior and exterior channels towards water transport in TFN membranes. Four types of TFN membranes incorporating silica-based NPs, i.e., hydrophilic vs. hydrophobic and porous vs. nonporous, were synthesized. Through the systematic evaluation of the physicochemical properties and separation performance of these membranes, we were able to determine the respective contributions to water permeance by the interior vs. exterior channels for the first time. Our work provides mechanistic insights into the formation and transport mechanisms to guide the future development of TFN membranes.

MATERIALS AND METHODS

Materials and chemicals.

Unless specified otherwise, all chemicals were analytical grade and purchased from Sigma-Aldrich. Deionized (DI) water for all solution preparation and filtration was made by Millipore Deionized (DI) system (Millipore, Billerica, MA). Tetraethyl orthosilicate (TEOS, 98%) and cetyltrimethylammonium bromide (CTAB, 95%) were used as silica precursor and surfactant, respectively. Aqueous ammonia solution (catalyst, 20–22%) obtained from Fisher Scientific was used for the preparation of the nonporous silica NPs. Dimethyldichlorosilane (DMDCS, ≥99.5%, Aldrich) was used to modify the silica surface to prepare the hydrophobic NPs. Polysulfone (PSF, pellets, Mw=35,000) and *N*, *N*-dimethylformamide (DMF, 99.8%) were used for fabricating the substrate. The interfacial polymerization process was performed by using *m*-phenylenediamine (MPD, >99%) in DI water and trimesoyl chloride (TMC, >98.5%) in hexane (HPLC, 95%).

Synthesis and modification of silica NPs.

Solid spherical silica NPs were synthesized through the hydrolysis of TEOS in ethanol with ammonia as a catalyst, and porous MCM-41 silica NPs were synthesized by using TEOS as silica source and CTAB as the surfactant. Detailed procedures could be found in our previous study.[19] The unmodified solid silica and MCM-41 were denoted as S and MCM, respectively.

Hydrophobic silica NPs were prepared by using a method obtained from the literature,[24] where the silanol groups on silica are replaced by DMDCS by surface modification. Briefly, the pristine silica NPs were immersed in DMDCS and stirred for 72 hr at room temperature. The ratio of DMDCS to silica was around 20 ml DMDCS per 100 m^2 of surface area for the silica NPs. The modified silica NPs was recovered from the Soxhlet extraction apparatus using 250 ml methanol. The modified silica NPs and MCM-41 were denoted as mS and mMCM, respectively.

Fabrication of TFC and TFN membranes.

Prior to the membrane fabrication, PSF substrates (15 wt% in DMF) were prepared by phase inversion based on our previous method.[25] To synthesis the TFC membrane, an IP reaction was performed on the PSF substrate. Briefly, the PSF substrate was immersed in an MPD/DI water solution (2 wt%) for 3 mins. The extra solution was removed by a rubber roller. Then, a TMC/hexane solution (0.15 wt%) was poured onto the MPD-saturated substrate to initiate the IP reaction. The reaction time was terminated after 2 mins by rinsing the membrane with hexane. Subsequently, the membrane was placed in an oven at 80 °C for 5 mins in order to enhance the cross-linking process. The membrane was then taken out and stored in DI water at 4 °C before use.

The synthesis procedure for TFN membranes was identical to that of TFC, except that different amounts of silica NPs varied from 0.01 to 0.1 wt.% were added into the

TMC/hexane solution before the IP reaction. The uniform dispersion of NPs in the TMC-hexane solution was achieved by ultrasonication for 1 h. The TFN membranes prepared in this study are denoted as TFN-X-n, where X stands for the type of nanofiller used (S, mS, MCM, or mMCM) and n stands for the wt% of the nanofiller used (0.01, 0.025, 0.05 or 0.1). The approach to disperse NPs in organic phase for fabricating TFN membrane has been well-documented in the literature.[11, 19, 26]

Material characterization and membrane performance tests.

Morphology of NPs was examined by TEM (JEOL 1400, JEOL Ltd., Peabody, MA). Prior to the characterization, the as-prepared NPs were dispersed in ethanol solution with sonication, and the NPs-ethanol solution was dropped onto a carbon-coated copper TEM grid with drying at room temperature. The crystalline structures of modified and unmodified MCM-41 (i.e., MCM and mMCM) were evaluated by fast Fourier transform (FFT) of a scanning transmission electron microscope (STEM, FEI Tecnai G2 20 S-TWIN). The specific surface areas, pore volume and pore size distribution of the NPs were evaluated by Brunauer–Emmett–Teller (BET) method and density functional theory (DFT) method, respectively, based on our previous work.[19] A scanning electron microscope (SEM) was applied to examine membrane surface morphology. To increase the conductivity of samples, all membrane specimens were coated with platinum using a sputter coater (20 mA, K575x, Emitech Ltd., Kent, England) for 1 min. The TEM cross-sections of the TFC and TFN membranes were prepared according to our previous study.[19, 27] Briefly, membrane

specimens were embedded in a resin (Eponate 12, Ted Pella, Inc., Redding, CA). The resin block was cut onto a copper grid in the thickness of 100 nm using an Ultracut E ultramicrotome (Reichert, Inc. Depew, NY) for TEM imaging.

Membrane surface functional groups were analyzed by attenuated total reflection Fourier transform infrared (ATR-FTIR), and hydrophilicity of the membrane surface were evaluated by contact angle measurement based on our previous work.[19, 25, 28] Membrane water flux and NaCl rejection were evaluated by a home-designed high-pressure cross-flow filtration system based on previous work.[19, 25, 28] Membrane water permeability coefficient A (L m^{-2} h^{-1} bar^{-1}) and salt permeability coefficient B (L m^{-2} h^{-1}) are calculated based on the references.[8, 29]

RESULTS AND DISCUSSION

Properties of pristine and modified NPs

TEM images (Figure 1a-d) show that both MCM and S had a near-spherical shape with comparable particle diameter (102.2 ± 9.8 nm vs. 105.7 ± 9.3 nm) and that the hydrophobic modification did not result in noticeable changes in their size and shape. Highly ordered hexagonal array and streak structure were observed for both the pristine MCM and the modified mMCM, corresponding to the interior channels of these porous nanofillers (Figure 1c,d) with mesopores of 3.5 - 3.6 nm in diameter based on their FFT patterns. In contrast, such interior structures were not observed for the solid NPs S and mS (Figure 1a,b). Figure 1e shows that the modified NPs mS and mMCM had significantly larger water contact angles (over 140°) compared to the respective values for their pristine counterparts S and MCM (less than 10°), confirming the successful hydrophobic modification by the surface grafting of DMDCS (also see the FTIR results in Supporting Information Figure S1).

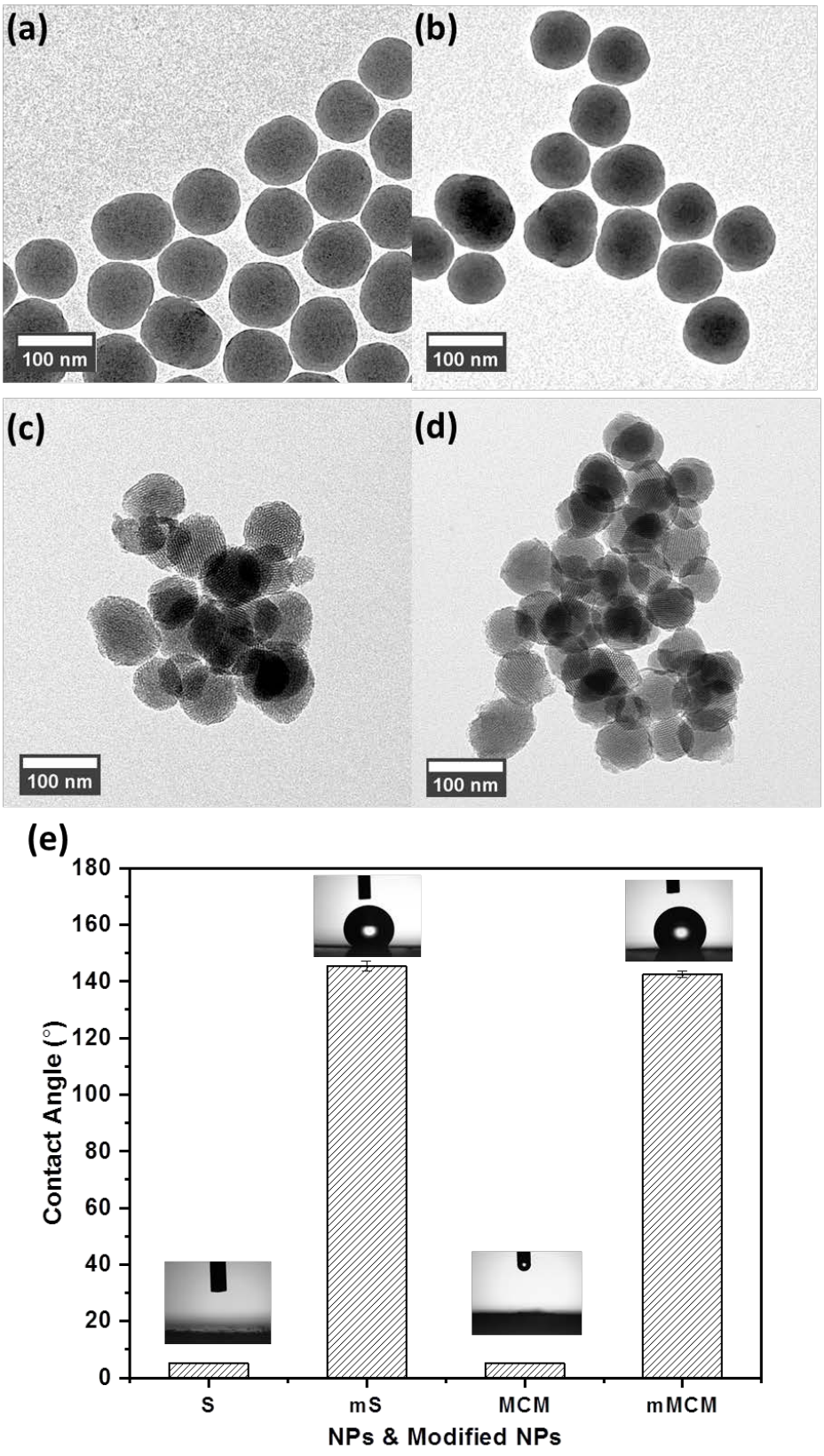

171

172 Figure 1. TEM images of (a) solid silica NPs (S); (b) modified solid silica NPs (mS); (c)
173 MCM-41 NPs (MCM); (d) modified MCM-41 NPs (mMCM); and (e) water contact angle
174 results. The scale bar for all TEM images is 100 nm.

Properties of TFC and TFN membranes.

FTIR results (Supporting information Figure S4) show the characteristic peaks at 1547 cm^{-1} (the Amide II band), 1663 cm^{-1} (amide I, C=O stretching vibrations of amide) and 1609 cm^{-1} (N-H stretching of amide) for both TFC and TFN membranes, confirming the formation of aromatic polyamide.[30] These membranes present rough surfaces with leaf-like morphologies (Supporting Information Figure S3) that are typical for polyamide-based RO membranes.[31, 32] Membrane surface hydrophilicity was affected by the embedded NPs (Supporting information Figure S5), with the hydrophilic NPs showing decreased water contact angles and the hydrophobic counterparts showing the opposite. The result can be due to the exposure of the aggregation of these NPs at the membrane's surface (Supporting information Figure S3), which is in good agreement with the literature.[33, 34]

TEM cross-sectional micrographs (Figure 2a-c) also show these roughness features, which are in concert with the SEM results. In addition, the TFN membranes TFN-MCM-0.05 (Figure 2b) and TFN-mMCM-0.05 (Figure 2c) show clearly the presence of MCM-41 NPs in the polyamide layer, confirming the successful incorporation of NPs. Interestingly, interfacial gaps can be clearly observed between the hydrophilic MCM-41 NPs and the polyamide matrix of the TFC-MCM-0.05 membrane (inset of Figure 2b), which was absent in the TFN-mMCM-0.05 embedded with hydrophobically modified MCM-41 NPs (Figure 2c). The interfacial gaps in TFC-MCM-0.05 can be attributed to the formation of exterior channels around the hydrophilic NPs during the IP reaction. According to the literature,[20, 35] hydrophilic

NPs can attract water molecules, which hydrolyzes TMC to inhibit the formation of polyamide in the vicinity of these particles and therefore generate exterior channels between NPs and the polyamide matrix in addition to any interior channels within the NPs.

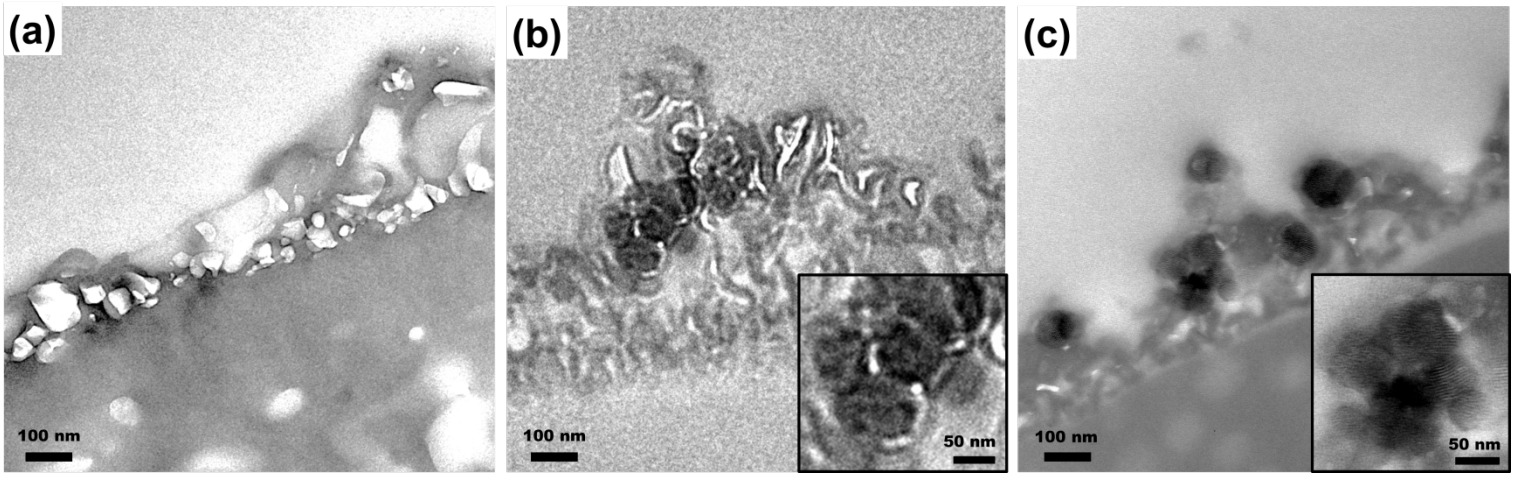

Figure 2. TEM cross-sections of (a) the control TFC, (b) TFN-MCM-0.05 and (c) TFN-mMCM-0.05 membranes. The scale bar for all TEM micrographs is 100 nm. Magnified images of the pristine and modified MCM-41 NPs-incorporated TFN membranes are inserted in the corresponding TEM micrographs with a scale bar of 50 nm.

Water transport properties of TFC and TFN membranes.

Figure 3a presents the water flux and NaCl rejection of TFN membranes incorporated with hydrophilic or hydrophobic nonporous silica NPs, with the membrane corresponding to 0 wt% NP loading representing the control TFC membrane. For the TFN-mS series, increasing the loading of hydrophobic nonporous silica NPs up to 0.1 wt% had no major change in membrane water flux and NaCl rejection. In contrast, the permeate flux increased significantly at increased loading of hydrophilic nonporous silica NPs for the TFN-S series (e.g., 34.5 L ± 1.8 L m^{-2} h^{-1} for the TFN-S-0.05 membrane vs. 28.2 ± 1.5 for the control TFC membrane, corresponding to a 22.2%

enhancement in flux). Compared to its TFN-mS counterpart, this enhancement in water flux for TFN-S can be ascribed to the formation of exterior nanochannels induced by the hydrophilic silica NPs, which serve as high permeability "aqueducts" to reduce the overall hydraulic resistance of the membrane.[20] The absence of both interior and exterior nanochannels of the TFN-mS membranes explains their inefficiency in enhancing membrane water permeance. Indeed, a few studies incorporating hydrophobic NPs[33, 36] even report reduced water permeance due to the blockage of water transport by these solid nanofillers.

Figure 3b shows that the NaCl rejection of TFN membranes incorporated with hydrophilic MCM NPs (the TFN-MCM series) or hydrophobically modified mMCM NPs (the TFN-mMCM series). The rejection was relatively constant at approximately 97-98%, regardless of the type and loading of NPs (Additional water/NaCl transport properties can be found in the Supporting Information Figure S6). On the other hand, increasing the loading of these porous nanofillers resulted in obviously higher water fluxes. The TFN-mMCM-0.05 membrane containing hydrophobic porous mMCM had a water flux of 35.2 L ± 2.1 L $m^{-2} h^{-1}$, which was 24.6% higher than that of the control TFC membrane. The enhancement in flux for the TFN-mMCM series is in direct contrast to the negligible effect for TFN-mS series. Therefore, we attribute this enhancement to the interior channels of the mMCM NPs, which could provide preferential pathways for water molecules.[11, 19] The replacement of mMCM nanofillers by their hydrophilic counterparts led to even greater enhancement in flux,

with the TFN-MCM-0.1 showing a flux of 46.6 L ± 1.1 L m^{-2} h^{-1} or 64.8% enhancement over the control, thanks to the combined effects of exterior channels (due to the hydrophilicity of the nanofillers) and interior channels of MCM NPs. However, the over-dosed NPs (e.g., at 0.1 wt%) could result in marginal water flux enhancement for the TFN membrane, and even some studies in the literature reported decreased water flux at higher NPs loading,[10, 37] potentially due to the severe NPs aggregation and the percolation threshold of dense polyamide rejection layer.

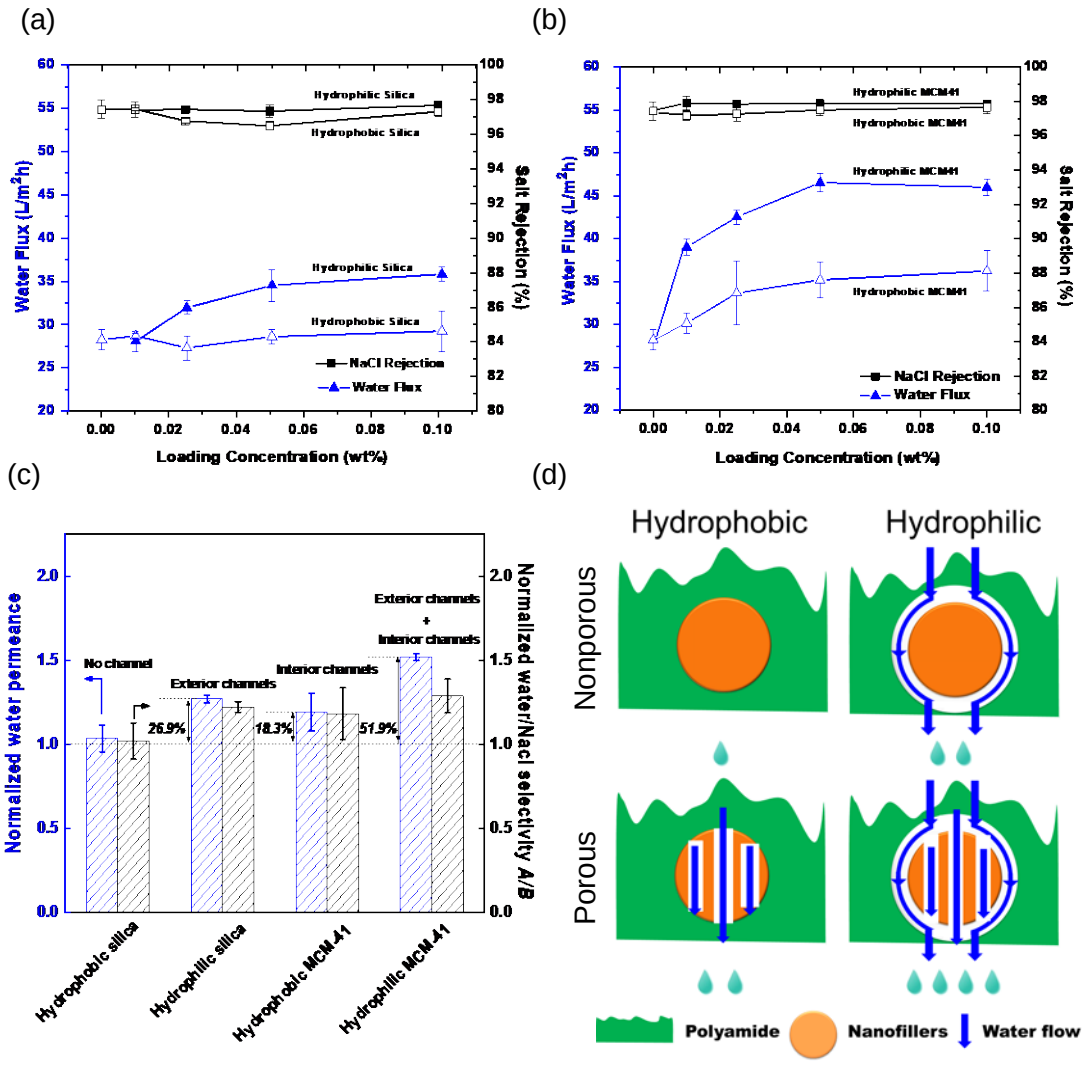

Figure 3. Membrane water flux and salt rejection of (a) TFN membranes with hydrophilic or hydrophobic nonporous silica NPs; (b) TFN membranes with hydrophilic or hydrophobic porous MCM-41, (c) normalized water permeability coefficient *A* and normalized water/NaCl selectivity *A*/*B* of the TFN membranes (at the same NPs number density of 48 #/μm^2, 0.1 wt% for TFN-(m)S and 0.025 wt% for TFN-(m)MCM, Supporting Information Figure S7) by the control TFC membrane and the NaCl rejection of the TFN membranes and (d) schematic diagram of the mechanism of hydrophilic silica or MCM-41 NPs induced nanochannels and hydrophobic silica and MCM-41 NPs in the polyamide layer for efficient water transport. The water flux and NaCl rejection results of TFN membranes with hydrophilic silica and hydrophilic MCM-41 were obtained from our previous study.[19] The experiments were performed under a transmembrane pressure of 300 psi at 25 °C using a 2000 ppm NaCl solution. All separation performances results are based on three replicate membranes.

It has long been debated in the literature what mechanism(s) could take credit for the enhanced separation performance of TFN membranes.[14, 38-41] In this study, we answered this question in a simple but elegant manner by systematically varying the properties of the nanofillers (porous vs. nonporous and hydrophilic vs. hydrophilic). We show that hydrophilic nanofillers performed better than their hydrophobic counterparts at the same number density of the loaded NPs (see TFN-S vs. TFN-mS and TFN-MCM vs. TFN-mMCM, Figure 3c and Supporting Information Figure S7), thanks to the exterior channels (or voids between NPs and polymer) induced by the hydrophilic NPs (Figure 3d and Refs.[11, 19, 20]). In addition, porous nanofillers had better permeability than their nonporous counterparts (see TFN-MCM vs. TFN-S and TFN-mMCM vs. TFN-mS, Figure 3c), underpinning the important role of interior channels for providing additional water pathways. Therefore, the current study offers convincing experimental evidence that both the exterior and interior channels contribute to enhancing the permeate flux of the corresponding TFN membranes.

These findings provide new insights into the advanced synthesis of TFN membranes for desalination and water reuse applications.

As shown in Figure 3c, at same number density of the loaded NPs, the exterior and interior channels appeared to have slightly different contributions to water flux enhancement (26.9% enhancement for exterior channels and 18.3% enhancement for interior channels). In addition to the absence of exterior channels, the slightly reduced flux enhancement of TFN-mMCM membrane can be potentially due to the possible formation of polyamide inside the NPs pores and the reduced pore volume of the mMCM NPs (Supporting Information, Figure S2). Obviously, these contributions would strongly depend on the properties of the nanofillers (e.g., the size, shape, orientation, distribution, concentration and hydrophilicity of the NPs and their pore size and structure). For example, NPs with high aspect ratios (e.g., nanofibers vs. nanospheres) present greater interfacial areas and may have better chances to creates more exterior channels.[42, 43] In this study, the orientation of the loaded (m)MCM NPs was random. Future study could explore the impact of pore orientation on affecting membrane separation performance. It is also interesting to note that the combined effects of both exterior and interior channels (TFN-MCM vs. the TFC control, 51.9% enhancement) were greater than the sum of their individual contributions (26.9 + 18.3%), suggesting a potential synergistic effect possibly due to the increased interconnectivity between these water channels. Furthermore, although the current study shows little effect of nanofillers on membrane rejection (possibly due to the

297 relatively small pores of ~3.5 nm in which electric double layer overlap could easily
298 occur), future studies need to further investigate the pore size of the interior channels
299 [44, 45] as well as the size of the induced exterior channels [20] on the selectivity of the
300 resulting TFN membranes.

ASSOCIATED CONTENT

The Supporting Information is available free of charge on the ACS Publications website at DOI:

S1. FTIR spectra and BET results of the pristine and modified silica and MCM-41 NPs; S2. SEM, FTIR and contact angle results of TFC and TFN membranes, S3. Water and NaCl transport properties in TFC and TFN membranes and S4. Supplementary information for membrane fabrication and characterization.

AUTHOR INFORMATION

Corresponding Author

*Phone: (+852) 2857 8470; E-mail address: zheyang@connect.hku.hk

*Phone: (+1) 573 882 0075; Email: dengb@missouri.edu

Notes

The authors declare no completing financial interest.

ACKNOWLEDGEMENTS

Financial support of this research was partially provided by the Missouri Water Resources Research Center (MWRRC). The Electron Microscopic Unit (EMU) at The University of Hong Kong was thanked for the TEM preparation and analysis.

REFERENCES

1. Tang, C. Y.; Yang, Z.; Guo, H.; Wen, J.; Nghiem, L. D.; Cornelissen, E. R., Potable water reuse through advanced membrane technology. *Environ. Sci. Technol.* **2018,** *52*, (18), 10215-10223.
2. Pendergast, M. M.; Hoek, E. M., A review of water treatment membrane nanotechnologies. *Energy Environ. Sci.* **2011,** *4*, (6), 1946-1971.
3. Elimelech, M.; Phillip, W. A., The future of seawater desalination: energy, technology, and the environment. *Science* **2011,** *333*, (6043), 712-717.
4. Yang, Z.; Ma, X.-H.; Tang, C. Y., Recent development of novel membranes for desalination. *Desalination* **2018,** *434*, 37-59.
5. Lee, K. P.; Arnot, T. C.; Mattia, D., A review of reverse osmosis membrane materials for desalination—development to date and future potential. *J. Membr. Sci.* **2011,** *370*, (1), 1-22.
6. Werber, J. R.; Osuji, C. O.; Elimelech, M., Materials for next-generation desalination and water purification membranes. *Nature Review Materials* **2016,** *1*, 16018.
7. Song, X.; Gan, B.; Qi, S.; Guo, H.; Tang, C. Y.; Zhou, Y.; Gao, C., Intrinsic Nanoscale Structure of Thin Film Composite Polyamide Membranes: Connectivity, Defects, and Structure-Property Correlation. *Environ. Sci. Technol.* **2020,** *54*, (6), 3559-3569.
8. Yang, Z.; Guo, H.; Tang, C. Y., The upper bound of thin-film composite (TFC) polyamide membranes for desalination. *J. Membr. Sci.* **2019,** *590*, 117297.
9. Geise, G. M.; Park, H. B.; Sagle, A. C.; Freeman, B. D.; McGrath, J. E., Water permeability and water/salt selectivity tradeoff in polymers for desalination. *J. Membr. Sci.* **2011,** *369*, (1), 130-138.
10. Yin, J.; Deng, B., Polymer-matrix nanocomposite membranes for water treatment. *J. Membr. Sci.* **2015,** *479*, 256-275.
11. Jeong, B.-H.; Hoek, E. M.; Yan, Y.; Subramani, A.; Huang, X.; Hurwitz, G.; Ghosh, A. K.; Jawor, A., Interfacial polymerization of thin film nanocomposites: a new concept for reverse osmosis membranes. *J. Membr. Sci.* **2007,** *294*, (1), 1-7.
12. Lind, M. L.; Ghosh, A. K.; Jawor, A.; Huang, X.; Hou, W.; Yang, Y.; Hoek, E. M. V., Influence of zeolite crystal size on zeolite-polyamide thin film nanocomposite membranes. *Langmuir* **2009,** *25*, (17), 10139-10145.
13. Ma, D.; Peh, S. B.; Han, G.; Chen, S. B., Thin-Film Nanocomposite (TFN) Membranes Incorporated with Super-Hydrophilic Metal–Organic Framework (MOF) UiO-66: Toward Enhancement of Water Flux and Salt Rejection. *ACS Appl. Mater. Interfaces* **2017,** *9*, (8), 7523-7534.
14. Dai, R.; Guo, H.; Tang, C. Y.; Chen, M.; Li, J.; Wang, Z., Hydrophilic Selective Nanochannels Created by Metal Organic Frameworks in Nanofiltration Membranes Enhance Rejection of Hydrophobic Endocrine-Disrupting Compounds. *Environ. Sci. Technol.* **2019,** *53*, (23), 13776-13783.
15. Zhao, Y.; Qiu, C.; Li, X.; Vararattanavech, A.; Shen, W.; Torres, J.; Helix-Nielsen, C.; Wang, R.; Hu, X.; Fane, A. G., Synthesis of robust and

high-performance aquaporin-based biomimetic membranes by interfacial polymerization-membrane preparation and RO performance characterization. *J. Membr. Sci.* **2012,** *423*, 422-428.
16. Qi, S.; Wang, R.; Chaitra, G. K. M.; Torres, J.; Hu, X.; Fane, A. G., Aquaporin-based biomimetic reverse osmosis membranes: Stability and long term performance. *J. Membr. Sci.* **2016,** *508*, 94-103.
17. Wang, C.; Li, Z.; Chen, J.; Li, Z.; Yin, Y.; Cao, L.; Zhong, Y.; Wu, H., Covalent organic framework modified polyamide nanofiltration membrane with enhanced performance for desalination. *J. Membr. Sci.* **2017,** *523*, 273-281.
18. Li, C.; Li, S.; Tian, L.; Zhang, J.; Su, B.; Hu, M. Z., Covalent organic frameworks (COFs)-incorporated thin film nanocomposite (TFN) membranes for high-flux organic solvent nanofiltration (OSN). *J. Membr. Sci.* **2019**, 520-531.
19. Yin, J.; Kim, E.-S.; Yang, J.; Deng, B., Fabrication of a novel thin-film nanocomposite (TFN) membrane containing MCM-41 silica nanoparticles (NPs) for water purification. *J. Membr. Sci.* **2012,** *423*, 238-246.
20. Yang, Z.; Guo, H.; Yao, Z.-k.; Mei, Y.; Tang, C. Y., Hydrophilic Silver Nanoparticles Induce Selective Nanochannels in Thin Film Nanocomposite Polyamide Membranes. *Environ. Sci. Technol.* **2019,** *53*, (9), 5301-5308.
21. Kim, E. S.; Hwang, G.; Gamal El-Din, M.; Liu, Y., Development of nanosilver and multi-walled carbon nanotubes thin-film nanocomposite membrane for enhanced water treatment. *J. Membr. Sci.* **2012,** *394-395*, 37-48.
22. Lee, H. S.; Im, S. J.; Kim, J. H.; Kim, H. J.; Kim, J. P.; Min, B. R., Polyamide thin-film nanofiltration membranes containing TiO2 nanoparticles. *Desalination* **2008,** *219*, (1-3), 48-56.
23. Rajaeian, B.; Rahimpour, A.; Tade, M. O.; Liu, S., Fabrication and characterization of polyamide thin film nanocomposite (TFN) nanofiltration membrane impregnated with TiO2 nanoparticles. *Desalination* **2013,** *313*, 176-188.
24. Pakizeh, M.; Moghadam, A. N.; Omidkhah, M. R.; Namvar-Mahboub, M., Preparation and characterization of dimethyldichlorosilane modified SiO2/PSf nanocomposite membrane. *Korean J. Chem. Eng.* **2013,** *30*, (3), 751-760.
25. Yin, J.; Yang, Y.; Hu, Z.; Deng, B., Attachment of silver nanoparticles (AgNPs) onto thin-film composite (TFC) membranes through covalent bonding to reduce membrane biofouling. *J. Membr. Sci.* **2013,** *441*, (Supplement C), 73-82.
26. Sorribas, S.; Gorgojo, P.; Téllez, C.; Coronas, J.; Livingston, A. G., High flux thin film nanocomposite membranes based on metal–organic frameworks for organic solvent nanofiltration. *J. Am. Chem. Soc.* **2013,** *135*, (40), 15201-15208.
27. Yang, Z.; Wu, Y.; Wang, J.; Cao, B.; Tang, C. Y., In situ reduction of silver by polydopamine: A novel antimicrobial modification of a thin-film composite polyamide membrane. *Environ. Sci. Technol.* **2016,** *50*, (17), 9543-50.
28. Yin, J.; Zhu, G.; Deng, B., Graphene oxide (GO) enhanced polyamide (PA) thin-film nanocomposite (TFN) membrane for water purification. *Desalination* **2016,** *379*, 93-101.

29. Gao, F.; Hunter, A.; Qu, S.; Hoffman, J. R.; Gao, P.; Phillip, W. A., Interfacial Junctions Control Electrolyte Transport through Charge-Patterned Membranes. *ACS Nano* **2019,** *13*, (7), 7655-7664.
30. Tang, C. Y.; Kwon, Y.-N.; Leckie, J. O., Effect of membrane chemistry and coating layer on physiochemical properties of thin film composite polyamide RO and NF membranes: I. FTIR and XPS characterization of polyamide and coating layer chemistry. *Desalination* **2009,** *242*, (1-3), 149-167.
31. Ma, X.-H.; Yao, Z.; Yang, Z.; Guo, H.; Xu, Z.; Tang, C. Y.; Elimelech, M., Nanofoaming of Polyamide Desalination Membranes to Tune Permeability and Selectivity. *Environ. Sci. Technol. Lett.* **2018,** *5*, (2), 123-130.
32. Lin, L.; Lopez, R.; Ramon, G. Z.; Coronell, O., Investigating the void structure of the polyamide active layers of thin-film composite membranes. *J. Membr. Sci.* **2016,** *497*, 365-376.
33. Pang, R.; Zhang, K., Fabrication of hydrophobic fluorinated silica-polyamide thin film nanocomposite reverse osmosis membranes with dramatically improved salt rejection. *J. Colloid. Interface Sci.* **2018,** *510*, 127-132.
34. Yang, Z.; Wu, Y.; Guo, H.; Ma, X.-H.; Lin, C.-E.; Zhou, Y.; Cao, B.; Zhu, B.-K.; Shih, K.; Tang, C. Y., A novel thin-film nano-templated composite membrane with in situ silver nanoparticles loading: Separation performance enhancement and implications. *J. Membr. Sci.* **2017,** *544*, 351-358.
35. Chan, W.-F.; Marand, E.; Martin, S. M., Novel zwitterion functionalized carbon nanotube nanocomposite membranes for improved RO performance and surface anti-biofouling resistance. *J. Membr. Sci.* **2016,** *509*, 125-137.
36. Yang, Z.; Huang, X.; Ma, X.-h.; Zhou, Z.-w.; Guo, H.; Yao, Z.; Feng, S.-P.; Tang, C. Y., Fabrication of a novel and green thin-film composite membrane containing nanovoids for water purification. *J. Membr. Sci.* **2019,** *570-571*, 314-321.
37. Yang, Z.; Yin, J.; Deng, B., Enhancing water flux of thin-film nanocomposite (TFN) membrane by incorporation of bimodal silica nanoparticles. *Aims Press Envrion. Sci.* **2016,** *3*, (2), 185-198.
38. Bai, L.; Liu, Y.; Bossa, N.; Ding, A.; Ren, N.; Li, G.; Liang, H.; Wiesner, M. R., Incorporation of Cellulose Nanocrystals (CNCs) into the Polyamide Layer of Thin-Film Composite (TFC) Nanofiltration Membranes for Enhanced Separation Performance and Antifouling Properties. *Environ. Sci. Technol.* **2018,** *52*, (19), 11178-11187.
39. Lind, M. L.; Suk, D. E.; Nguyen, T. V.; Hoek, E. M. V., Tailoring the structure of thin film nanocomposite membranes to achieve seawater RO membrane performance. *Environ. Sci. Technol.* **2010,** *44*, (21), 8230-8235.
40. Valentino, L.; Matsumoto, M.; Dichtel, W. R.; Marinas, B. J., Development and Performance Characterization of a Polyimine Covalent Organic Framework Thin-Film Composite Nanofiltration Membrane. *Environ. Sci. Technol.* **2017,** *51*, (24), 14352-14359.
41. Rahimpour, A.; Seyedpour, S. F.; Aghapour Aktij, S.; Dadashi Firouzjaei, M.; Zirehpour, A.; Arabi Shamsabadi, A.; Khoshhal Salestan, S.; Jabbari, M.; Soroush, M., Simultaneous Improvement of Antimicrobial, Antifouling, and Transport Properties

of Forward Osmosis Membranes with Immobilized Highly-Compatible Polyrhodanine Nanoparticles. *Environ. Sci. Technol.* **2018,** *52*, (9), 5246-5258.
42. Liu, S.; Low, Z.-X.; Hegab, H. M.; Xie, Z.; Ou, R.; Yang, G.; Simon, G. P.; Zhang, X.; Zhang, L.; Wang, H., Enhancement of desalination performance of thin-film nanocomposite membrane by cellulose nanofibers. *J. Membr. Sci.* **2019,** *592*, 117363.
43. Sun, Z.; Wu, Q.; Ye, C.; Wang, W.; Zheng, L.; Dong, F.; Yi, Z.; Xue, L.; Gao, C., Nanovoid Membranes Embedded with Hollow Zwitterionic Nanocapsules for a Superior Desalination Performance. *Nano Lett.* **2019**.
44. Van Goethem, C.; Verbeke, R.; Hermans, S.; Bernstein, R.; Vankelecom, I. F. J., Controlled positioning of MOFs in interfacially polymerized thin-film nanocomposites. *J. Mater. Chem. A* **2016,** *4*, (42), 16368-16376.
45. Kadhom, M.; Deng, B., Metal-organic frameworks (MOFs) in water filtration membranes for desalination and other applications. *Appl. Mater. Today* **2018,** *11*, 219-230.